



## Synthesis and Characterization of Mesoporous Nano-Structured Mixed Metal Oxides

Amit Kumar<sup>\*1</sup>, Dibyarup Majumdar<sup>2</sup>, Shailey Singhal<sup>1</sup>, Shilpi Agarwal<sup>1</sup>, R. P. Badoni<sup>2</sup>, K. Mohan Reddy<sup>1</sup>

<sup>1</sup>Dept of Chemistry, College of Engineering Studies, University of Petroleum & Energy Studies, Dehradun, Uttarakhand, India.

<sup>2</sup>Dept of Chemical Engineering, College of Engg Studies, University of Petroleum & Energy Studies, Dehradun, Uttarakhand, India.

\*Corresponding author's E-mail: amitupes01@gmail.com

Accepted on: 12-12-2015; Finalized on: 31-08-2016.

### ABSTRACT

The aim of this study is to synthesize high surface area structured oxides, which can behave as good support for various catalytic reactions. Structured oxides were developed by sol-gel method by the intercalation of silica with other metal oxides, viz. alumina, zirconia and titania. The properties of structured oxides were examined using FE-SEM, PXRD, BET and ammonia TPD studies. All the structured oxides were mesoporous in nature with BET surface area in the range 325-390m<sup>2</sup>/g and pore size in the range 4.3-5.2nm. The evaluation indicated the formation of nano-structured oxides with average particle size range 12-18nm. The total acidity of the oxides ranged from 0.07-0.2 mmole/g.

**Keywords:** BET, nano-structured oxides, mixed oxides, nanoparticles.

### INTRODUCTION

Mixed-metal oxide systems are of great significance and are generated by the interaction of materials at the atomic level. Such systems have the potential for exhibiting chemical properties that differ notably from those of the corresponding single component oxides. They possess high catalytic suitability and thermal stability than the single component. In addition, they generate new surface acid sites to participate in the reaction. Owing to their excellent properties, mixed metal oxides are attracting considerable attention as advanced materials for various applications, one of the very important being as supports for heterogeneous catalysts. Mixed oxide systems are found to be highly efficient for acid-catalyzed reactions such as phenol amination<sup>1</sup>, ethene hydration<sup>1</sup>, butene isomerization<sup>1-3</sup>, cumene dealkylation<sup>4</sup>, 2-propanol dehydration<sup>4</sup> and 1, 2-dichloroethane decomposition<sup>5</sup>. The structure of mixed zirconia-silica oxides is very interesting because zirconium cannot substitute silicon, due to the different atomic radius and coordination number between these two elements. Thus, zirconia will develop as distinct phase in the nanocomposites, the formation of only monoclinic zirconia<sup>6</sup>.

Zirconia-containing mesoporous frameworks have been explored for both catalytic and adsorptive desulfurization. Kwon and coworkers showed 20% greater sulfur adsorption for a mesoporous silica/zirconia material compared to the pure silica version, even though the latter had a higher surface area<sup>7</sup>.

Klein have reported sol-gel-prepared TiO<sub>2</sub>-SiO<sub>2</sub> amorphous solids in which the surface polarity was modified by partial methylation of the surface of silica through the use of Si(OMe)<sub>3</sub>Me precursor, the surface polarity can affect not only the reaction rate and the

selectivity but also the overall conversion and catalyst lifetime<sup>8</sup>.

Selection of the synthesis procedure gives the prospect to synthesize high surface area mixed oxides with a wide variety of compositions and pore structures. Various strategies have been developed for the synthesis of oxides, which typically include co-precipitation<sup>1-2, 4</sup>, flame hydrolysis<sup>9</sup> and sol-gel hydrolysis<sup>10-11</sup>. In the present paper, we have prepared a series of mixed oxides by sol-gel method and the oxides were characterized by various techniques as Fourier transform infrared (FTIR), powdered X-ray diffraction (PXRD), scanning electron microscopy (SEM) etc. in order to illustrate their structure. The surface properties were evaluated by Brunauer-Emmett-Teller (BET) and ammonia temperature programmed-desorption (TPD) in order to study the surface area, pore size, pore volume and total acidity.

### MATERIALS AND METHODS

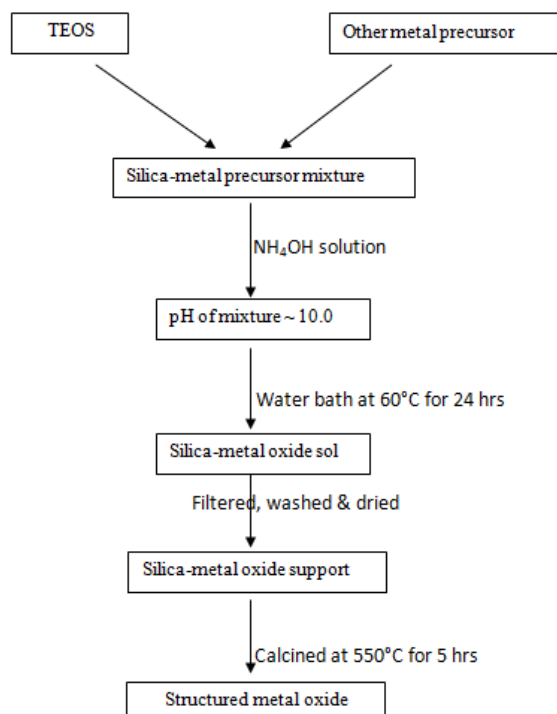
Fresh solutions were employed for all synthesis work. Tetraethyl orthosilicate (TEOS) was purchased from Sigma Aldrich, while Aluminium nitrate [Al(NO<sub>3</sub>)<sub>3</sub>] from Fisher Scientific. Zirconium oxychloride (ZrOCl<sub>2</sub>·8H<sub>2</sub>O) and titanium chloride (TiCl<sub>4</sub>) were of SDFine. All the chemicals were of AR grade. Ethanol used was of analytical grade (China) and ammonium hydroxide was supplied by SD fine chemicals, India.

### Synthesis of Structured Oxides

Structured oxides were synthesized by sol-gel method. For all the structured oxides, TEOS was used as precursor for silica. In a flat bottom flask, TEOS was diluted two times with ethanol and stirred vigorously for 15 minutes at room temperature. Dilute solution of precursor for other metal was then added slowly with continuous



stirring. The resulting solution was precipitated by the drop-wise addition of ammonium hydroxide until pH 10 and then kept in water bath at 60°C for 24 hr. The resulting mixed oxide gel was carefully filtered under vacuum, washed with distilled water followed by drying at room temperature overnight, followed by at 120°C for 12 hrs. The product was calcined at 550°C for 5 hours at ramp rate of 40°C/hr. The complete flow scheme for the synthesis of structured oxides is given in Scheme-1.



**Scheme 1:** Sol-gel Method for the Synthesis of Structured Metal Oxide

Three different structured oxides ( $\text{SiO}_2\text{-Al}_2\text{O}_3$ ,  $\text{SiO}_2\text{-ZrO}_2$  and  $\text{SiO}_2\text{-TiO}_2$ ) were synthesized in a ratio of 70:30. Details of precursor and experimental set up are described in Table-1.

### Characterization

The surface morphology of the structured oxides was characterized by Field emission scanning electron microscopy (Fe-SEM, SERON Technology, Korea) on 1  $\mu\text{m}$  and 5  $\mu\text{m}$  using 20 KVA on a magnification of 2x. The powder X-ray diffraction patterns were measured on Rigaku XPert Pro X-ray diffractometer and  $\text{CuK}\alpha 2$  contribution was eliminated by DIFFRAC/AT software ( $\text{CuK}\alpha$  radiation with  $\lambda = 1.541 \text{ \AA}$ ). Fourier transform infrared spectroscopy (FTIR; Perkin Elmer) was performed to examine the linkages between silica and heterometal oxide network. The Brunauer-Emmett-Teller (BET) surface area, pore size distributions, pore volumes, and average particle size was measured by nitrogen adsorption at 75 K using Accelerated Surface Area and Porosimetry System, Micromeritics, ASAP 2020. All the samples were degassed at 250°C for 6 hours prior to actual measurements.

The profile of temperature-programmed desorption of ammonia ( $\text{NH}_3\text{-TPD}$ ) over the catalysts was carried out in

a U type quartz reactor (ID = 6 mm) packed with about 0.1 g catalyst with a Micromeritics Chemisorb 2750. The samples were pre-treated for two hours at 150°C, under argon flow of  $20 \text{ ml min}^{-1}$  followed by cooling to room temperature in order to remove any physisorbed impurity on the surface of the sample. After pre-treatment, the samples were subjected to chemisorption step using ammonia in helium (9.8%, mol/mol) flow of  $20 \text{ ml min}^{-1}$  at room temperature, for 30 minutes. Thereafter, the system was purged with helium at room temperature for two hours. In order to remove extra ammonia molecules, the material was treated for 30 minutes at 120°C under helium flow ( $20 \text{ ml min}^{-1}$ ). This step was followed by thermal programmed desorption analysis, in which the sample was heated from 100 to 600°C, at a rate of  $10^\circ\text{C min}^{-1}$  and under helium flow ( $20 \text{ ml min}^{-1}$ ). The amount of desorbed ammonia was detected with thermal conductivity detector. The strength of the material was analyzed in terms of bulk density by pore filling method.

## RESULTS AND DISCUSSION

### Morphology and X-Ray Diffraction

#### SEM analysis

All the samples (before and after calcination) were colorless. Surface morphology and nature of oxides was investigated by scanning electron microscopy. Typical SEM photographs are given in Figure 1. From SEM images it can be seen that the morphology changes with the addition of another metal oxide to silica is observed in all the samples with respect the grain size and particles distributed with irregular in shape corresponding to the different metal oxide particles, in the case of  $\text{Al}_2\text{O}_3$  particles are appeared to be hallow in shape, and in the case of zirconia particles are irregular geometry and whereas in the case of titania particles are appeared to be spherical grains, which on aggregates with irregular shapes and uniform distribution as the silica composition is large in quantity.

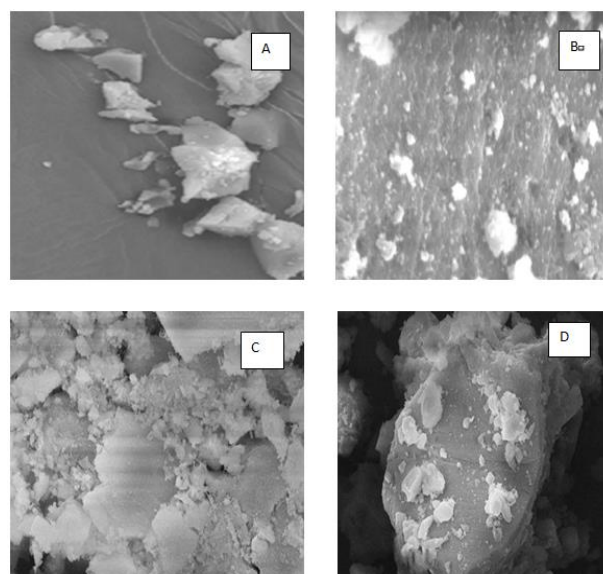


**Figure 1:** Fe-SEM image of samples (a) Pure silica (b)  $\text{SiO}_2\text{-Al}_2\text{O}_3$  (c)  $\text{SiO}_2\text{-ZrO}_2$  (d)  $\text{SiO}_2\text{-TiO}_2$

### PXRD Characterization

The PXRD pattern of pure silica,  $\text{SiO}_2\text{-Al}_2\text{O}_3$ ,  $\text{SiO}_2\text{-ZrO}_2$  and  $\text{SiO}_2\text{-TiO}_2$ , dried at  $550^\circ\text{C}$  were studied.

There is a new line in the PXRD patterns of (a), (b), (c) as shown in the Figure 2, when compared to the pure silica PXRD pattern of (d), which may be due to the generation of interlinkages between the two oxides. Sharp line at  $2\theta = 28^\circ$  is due to the incorporation of other metal oxide on silica network. Other lines with variable intensities at different  $2\theta$  values are observed in pattern (a) at  $2\theta = 46^\circ$ ,  $68^\circ$  and slight changes are observed for other patterns of (b) and (c).

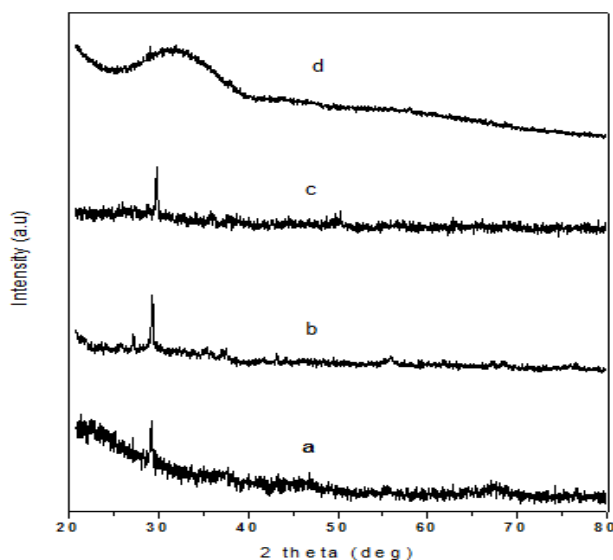


**Figure 2:** XRD patterns of (a)  $\text{SiO}_2\text{-Al}_2\text{O}_3$ , (b)  $\text{SiO}_2\text{-ZrO}_2$ , (c)  $\text{SiO}_2\text{-TiO}_2$ , (d) pure  $\text{SiO}_2$

### Fourier Transform Infrared Spectroscopy (FTIR)

FTIR graphs for structured oxides are reflected in Figure 3. Sharp peak at  $1632\text{cm}^{-1}$  in the spectrum of pure silica marks the presence of H-O-H bending vibration of water<sup>12</sup>.

Peak at  $1111\text{cm}^{-1}$  reflects asymmetric stretching of Si-O-Si;  $820\text{cm}^{-1}$  indicates symmetric stretching of Si-O-Si<sup>13-16</sup>.

Decrease in the intensity of  $1111\text{cm}^{-1}$  in structured oxides indicates the involvement of silica in linkage with other metals.

Among the FTIRs of structured oxides, occurrence of peak at  $1088\text{cm}^{-1}$  corresponds to Si-O-Al bonding<sup>17</sup> in Si-Al oxide and at  $1075\text{cm}^{-1}$  for Si-O-Zr<sup>18</sup> in Si-Zr oxide, confirming the synthesis of structured oxides.

Occurrence of new peak at  $969\text{cm}^{-1}$  is the characteristic of Si-O-Ti bridge in the structure<sup>13-14</sup>. Based upon the linkages present, it is very well confirmed that Si-O-M (where, M = Al, Zr, Ti) linkage exists in the structured oxides (Figure 4).

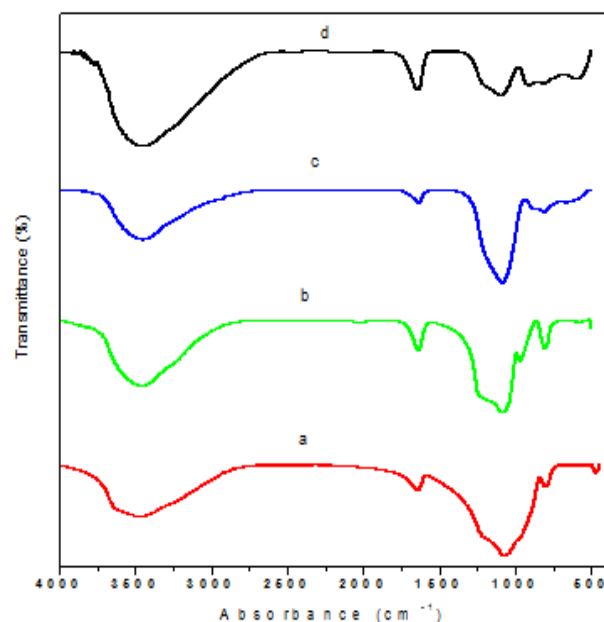


**Figure 3:** FTIR of samples (a)  $\text{SiO}_2\text{-ZrO}_2$  (b)  $\text{SiO}_2\text{-TiO}_2$  (c)  $\text{SiO}_2\text{-Al}_2\text{O}_3$  (d) Pure silica

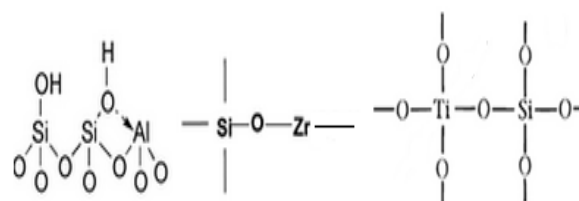


**Figure 4:** Skeletal structures of structured oxides

### $\text{N}_2$ Adsorption - Desorption Studies

$\text{N}_2$  adsorption-desorption isotherms for structured oxides are given in Figure 5a. Well defined hysteresis loops were obtained for all the samples. The occurrence of conspicuous hysteresis loops at high relative pressures indicates the presence of mesoporous material, being related to capillary condensation associated with large pore channels<sup>19</sup>. Among the synthesized structured oxides, it has been observed that the relative pressure point (where adsorption and desorption branches coincide) is affected by the type of the metal oxide present with  $\text{SiO}_2$ . Pure  $\text{SiO}_2$  showed hysteresis at highest relative pressure, showing the presence of maximum pore volume. Among various structured oxides,  $\text{SiO}_2\text{-ZrO}_2$  was found to have hysteresis at highest relative pressure, followed by  $\text{SiO}_2\text{-Al}_2\text{O}_3$  (slightly lower than  $\text{SiO}_2\text{-ZrO}_2$ ) and then  $\text{SiO}_2\text{-TiO}_2$ . Thus, it can be inferred that the pore volume decreased during the process of synthesizing structured oxides, which was further confirmed by pore size distribution (PSD). The PSD of the final products indicate that  $\text{SiO}_2\text{-TiO}_2$  has a wider PSD than  $\text{SiO}_2\text{-Al}_2\text{O}_3$  and  $\text{SiO}_2\text{-ZrO}_2$ . The intercalation of oxides and reduction of particle size to nano range could help in achieving high surface area with appreciable pore volume. The surface area of structured oxides in the order:  $\text{SiO}_2\text{-TiO}_2$  ( $388\text{m}^2/\text{g}$ ) >  $\text{SiO}_2\text{-ZrO}_2$  ( $364\text{m}^2/\text{g}$ ) >  $\text{SiO}_2\text{-Al}_2\text{O}_3$  ( $325\text{m}^2/\text{g}$ ),

however pore volume is maximum in case of  $\text{SiO}_2\text{-ZrO}_2$  (0.62cc/g).

Bulk density is an indicative of the strength of the material, which was contributed by both silica and other metal moiety; however acidity was mainly due to the incorporation of aluminium, zirconium and titanium moiety in the samples. The BET surface area, pore volume (Vp), average pore diameter, average particle size, total acidity and bulk density of the structured oxides are given in Table-2.

### Ammonia Absorption

The absorption of ammonia ( $\text{NH}_3$ -TPD) on the supports prepared was performed to obtain the acidity of the surface. The amounts of ammonia desorbed are plotted in Figure 6. The results show different extent of ammonia absorbed for the structured oxides. In  $\text{NH}_3$ -TPD profile, peaks generally are distributed into two regions, high temperature (HT) region ( $T > 400^\circ\text{C}$ ) recognizing the desorption of ammonia from strong acid sites and low

temperature (LT) region ( $T < 400^\circ\text{C}$ ) recognizing the desorption of ammonia from weak acid sites<sup>20,21</sup>.

TPD profile for all the samples were taken from 100–650 $^\circ\text{C}$  (Figure 6). All the samples displayed peaks between 100 to 500 $^\circ\text{C}$ .

The desorption peaks of TPD profiles located at 100–200 $^\circ\text{C}$ , 200–400 $^\circ\text{C}$  and 400–500 $^\circ\text{C}$  can be assigned to weak, moderate and strong acid sites, respectively<sup>22-24</sup>. Peak above 500 $^\circ\text{C}$  corresponded to the decomposition of strongly absorbed ammonia to nitrogen.

Total acidity of the samples is given in Table-2. Aluminium being most acidic in nature provided maximum acidity to oxides. Pure  $\text{SiO}_2$  contained 2.5mmol/g total acidity. While the  $\text{SiO}_2\text{-Al}_2\text{O}_3$ ,  $\text{SiO}_2\text{-ZrO}_2$  and  $\text{SiO}_2\text{-TiO}_2$  catalyst prepared in over study contained 6.38, 5.04, 4.01 mmol/g total acidity respectively. Thus, from these values the order of total acidity of these mixed metal oxides is given by  $\text{SiO}_2\text{-Al}_2\text{O}_3 > \text{SiO}_2\text{-ZrO}_2 > \text{SiO}_2\text{-TiO}_2$ .

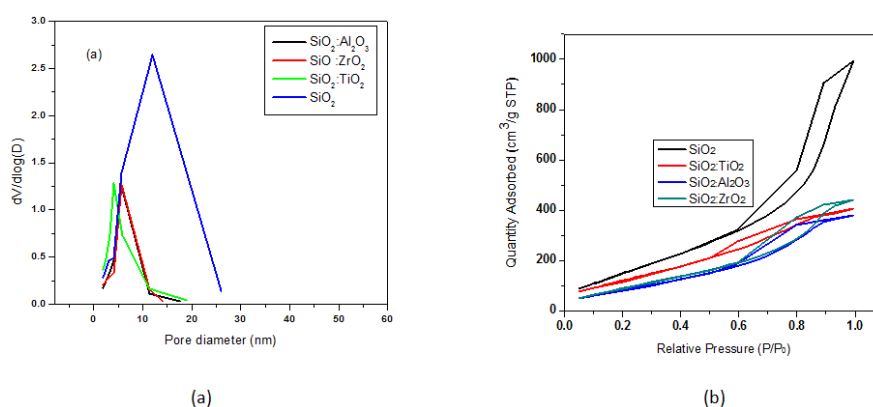


Figure 5: (a)  $\text{N}_2$  adsorption/desorption isotherms (b) Pore size distribution of samples

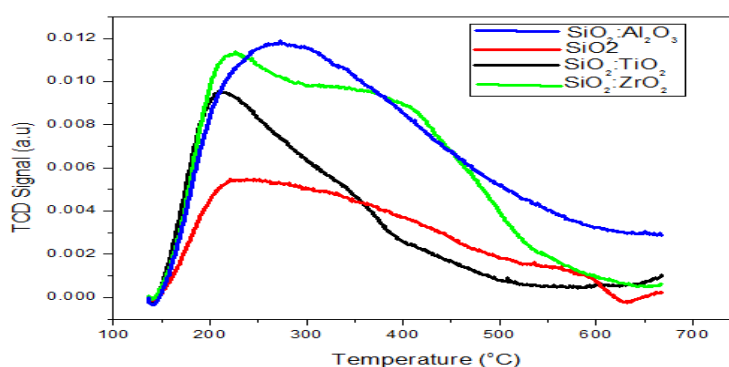


Figure 6: Ammonia desorption pattern of Structured Oxides and Pure Silica

Table 1: Details of Precursors for Structured Oxides

Structured oxide	Composition	Component	Precursor	Amount of Precursor	Solvent (ml)
$\text{SiO}_2\text{-Al}_2\text{O}_3$	70:30	$\text{SiO}_2$	TEOS	65 ml	65ml
		$\text{Al}_2\text{O}_3$	$\text{Al}(\text{NO}_3)_3$	55.16g	110ml
$\text{SiO}_2\text{-ZrO}_2$	70:30	$\text{SiO}_2$	TEOS	65 ml	65ml
		$\text{ZrO}_2$	$\text{ZrOCl}_2 \cdot 8\text{H}_2\text{O}$	19.5g	39ml
$\text{SiO}_2\text{-TiO}_2$	70:30	$\text{SiO}_2$	TEOS	65 ml	65ml
		$\text{TiO}_2$	$\text{TiCl}_4$	10.48ml	21ml



**Table 2:** Characteristics of Structured Oxides

Sample	S <sub>A</sub> (m <sup>2</sup> /g)	V <sub>P</sub> (cc/g)	D <sub>P</sub> (nm)	S <sub>P</sub> (nm)	A <sub>T</sub> (ml/g)	D <sub>B</sub> (g/cc)	Crystallinity
Pure SiO <sub>2</sub>	578	1.7	10.0	11.0	2.50	0.2	Amorphous
SiO <sub>2</sub> -Al <sub>2</sub> O <sub>3</sub>	325	0.54	5.02	15.80	6.38	0.53	Slightly crystalline
SiO <sub>2</sub> -ZrO <sub>2</sub>	364	0.62	5.19	17.36	5.04	0.52	Slightly crystalline
SiO <sub>2</sub> -TiO <sub>2</sub>	388	0.51	4.33	12.25	4.01	0.54	Slightly crystalline

S<sub>A</sub>: Surface area, V<sub>P</sub>: Pore volume, D<sub>P</sub>: Average pore diameter, S<sub>P</sub>: Average particle size, A<sub>T</sub>: Total acidity, D<sub>B</sub>: Bulk density.

## CONCLUSION

Nano-structured oxides of silica and heterometal (SiO<sub>2</sub>-Al<sub>2</sub>O<sub>3</sub>, SiO<sub>2</sub>-ZrO<sub>2</sub> and SiO<sub>2</sub>-TiO<sub>2</sub>) have been prepared by sol-gel method. Results indicate the viability of the method to obtain mesoporous structured oxides with larger pores. Variations in the metal combinations affected the characteristics of the oxides and incorporation of Al<sub>2</sub>O<sub>3</sub>, ZrO<sub>2</sub> and TiO<sub>2</sub> influenced the texture, structure and morphology of the samples. All the nano-structured oxides comprised of high surface area, good pore volume and acceptable acidity and bulk density. The surface area of structured oxides in the order: SiO<sub>2</sub>-TiO<sub>2</sub> (388m<sup>2</sup>/g) > SiO<sub>2</sub>-ZrO<sub>2</sub> (364m<sup>2</sup>/g) > SiO<sub>2</sub>-Al<sub>2</sub>O<sub>3</sub> (325m<sup>2</sup>/g), however pore volume is maximum in case of SiO<sub>2</sub>-ZrO<sub>2</sub> (0.62cc/g). It is important to mention that high surface area is the foremost required characteristic of an effective catalyst. In summary the order of total acidity of these mixed metal oxides is given by SiO<sub>2</sub>-Al<sub>2</sub>O<sub>3</sub> > SiO<sub>2</sub>-ZrO<sub>2</sub> > SiO<sub>2</sub>-TiO<sub>2</sub>. Hence acidity of the oxides is in lower range, but being associated with high surface area the synthesized nano-structured oxides can be a good choice to be used as support material for various catalytic reactions. This will help the active ingredient to disperse uniformly resulting in a suitable catalyst with required characteristics for a particular reaction.

**Acknowledgement:** Authors feel great pleasure to express their inexplicable & deep sense of gratitude to the Chancellor Dr. S. J. Chopra, Vice Chancellor Dr. Shrihari Honwad and Head, Department of Chemistry Dr. Pankaj Kumar for their continuous support and encouragement.

## REFERENCES

- Itoh M, Hattori H, Tanabe K. The acidic properties of TiO<sub>2</sub>-SiO<sub>2</sub> and its catalytic activities for the amination of phenol, the hydration of ethylene and the isomerization of butane, *J. Catal.* 35, 1974, 225-231.
- KO EI, Chen JP, Weissman JG. A study of acidic titania/silica mixed oxides and their use as supports for nickel catalysts, *J. Catal.* 105, 1987, 511-520.
- Gaube J, Klein HF. Kinetics and mechanism of butene isomerization/hydrogenation and of 1, 3-butadiene hydrogenation on palladium, *App. Catal. A: Gen.* 470, 2014, 361-368.
- JR Sohn, HJ Jang. Correlation between the infrared band frequency of the silanol bending vibration in TiO<sub>2</sub>-SiO<sub>2</sub> catalysts and activity for acid catalysis, *J. Catal.* 132, 1991, 563-565.
- Imamura S, Tarumoto H, Ishida S. Decomposition of 1,2-dichloroethane on titanium dioxide/silica, *Ind. Eng. Chem. Res.* 28(10), 1989, 1449-1452.
- Tahir A, Othman M. The development and characterization of Zirconia-Silica sand nanoparticles composites, *World journal of Nanoscience and Engineering.* 1, 2011, 7-14.
- Palomino JM, Tran DT, Kareh AR, Miller CA, Gardner JMV, Dong H, Oliver SRJ. Zirconia-silica based mesoporous desulfurization adsorbents', *J of power sources*, 278, 2015, 141-148.
- Kwon JM, Moon JH, Bae YS, Lee DG, Sohn HC, Lee CH, *Chem-Sus Chem*, 1, 2008, 307-309.
- Greeger RB, Lytle FW, Sandstrom DR, Wong J, Schultz P. Investigation of TiO<sub>2</sub>-SiO<sub>2</sub> glasses by X-ray absorption spectroscopy, *J. Non-Cryst. Solids*, 55, 1983, 27-43.
- Marth MS, Walther KL, Wokaun A, Handy BE, Baiker A. Porous silica gels and TiO<sub>2</sub>/SiO<sub>2</sub> mixed oxides prepared via the sol gel process: characterization by spectroscopic techniques, *J. Non-Cryst. Solids*, 143, 1992, 93-111.
- Walther KL, Wokaun A, Handy BE, Baiker A. TiO<sub>2</sub>/SiO<sub>2</sub> mixed oxide catalysts prepared by sol-gel techniques. Characterization by solid state CP/MAS spectroscopy, *J. Non-Cryst. Solids*, 134, 1991, 47-57.
- Pickup DM, Mountjoy G, Wallidge GW, Newport RJ, Smith ME. Structure of (ZrO<sub>2</sub>)<sub>x</sub>(SiO<sub>2</sub>)<sub>1-x</sub> xerogels (x = 0.1, 0.2, 0.3 and 0.4) from FTIR, 29Si and 17O MAS NMR and EXAFS, *Phys. Chem. Chem. Phys.* 1, 1999, 2527-2533.
- Shafei ELGMS, Mohamed MM, Interaction between molybdena and silica: FT-IR/PA studies of surface hydroxyl groups and pore structure assessment, *Colloids and surfaces A*, 94, 1995, 267-277.
- Mohamed MM, Salama TM, Yamaguchi T, Synthesis, characterization and catalytic properties of titania silica catalysts, *Colloids and Surfaces A: Physicochemical and Engineering Aspects*, 207, 2002, 25-32.
- Wu ZG, Zhao YX, Liu DS. The synthesis and characterization of mesoporous silica zirconia aerogels, *Microporous Mesoporous Mater*, 68(1-3), 2004, 127-132.
- Ma YY, Jia PN, Li XC, Liu N, Ma YL. Synthesis of the ZrO<sub>2</sub>-SiO<sub>2</sub> microspheres as a mesoporous candidate material, *J. Porous Mater*, 19(6), 2012, 1047-1052.
- Karakassides MA, Gournis D, Petridis D. An Infrared Reflectance Study of Si-O Vibrations in Thermally Treated



- Alkali-Saturated Montmorillonites, *Clay Minerals*, 34, 1999, 429-438.
18. Phillips JC, Thorpe MF. *Phase Transitions and Self-Organization in Electronic and Molecular Networks*, edited by, Springer, page 201.
  19. Sing KSW, Everett DH, Haul RAW, Moscou L, Pierotti RA, Rouquerol J, Siemieniowska T. Reporting physisorption data for gas/solid systems with special reference to the determination of surface area and porosity, *Pure Appl Chem*, 57(4), 1985, 603-619.
  20. Lonyl F and Valyon. On the interpretation of the NH<sub>3</sub>-TPD patterns of H-ZSM-5 and H-mordenite, *Microporous Mesoporous Mater*, 47, 2001, 293-301.
  21. Sawa M, Niwa M, Murakami Y. Relationship between acid amount and framework alumi-num content in mordenite', *Zeolites*, 10, 1990, 532-538.
  22. Wang S, Zhao L, Wang W, Zhao Y, Zhang G, Ma X, Gong J. Morphology control of ceria nanocrystals for catalytic conversion of CO<sub>2</sub> with methanol, *Nanoscale*, 5, 2013, 5582-5588.
  23. Itoh M, Hattori H, Tanabe K. The acidic properties of TiO<sub>2</sub>-SiO<sub>2</sub> and its catalytic activities for the amination of phenol, the hydration of ethylene and the isomerization of butene, *J. Catal*, 35, 1974, 225-231.
  24. Bosman HJM, Kruissimk EC, Spoel JVD, Brink F.V D. Characterization of the acid strength of SiO<sub>2</sub>-ZrO<sub>2</sub> mixed oxides, *J.Cat*, 148, 1994, 660-672.

**Source of Support: Nil, Conflict of Interest: None.**

